ACS APPLIED MATERIALS & INTERFACES

LETTER

www.acsami.org

Coating Alumina on Catalytic Iron Oxide Nanoparticles for Synthesizing Vertically Aligned Carbon Nanotube Arrays

Xin Wang,[†] Peter J. Krommenhoek,[†] Philip D. Bradford,[‡] Bo Gong,[§] Joseph B. Tracy,[†] Gregory N. Parsons,[§] Tzy-Jiun M. Luo,[†] and Yuntian T. Zhu*[,†]

[†]Department of Material Science and Engineering, [‡]Department of Textile Engineering, Chemistry and Science, and [§]Department of Chemical and Biomolecular Engineering, North Carolina State University, Raleigh, North Carolina 27695, United States

ABSTRACT: To synthesize long and uniform vertically aligned carbon nanotube (VACNT) arrays, it is essential to use catalytic nanoparticles (NPs) with monodisperse sizes and to avoid NP agglomeration at the growth temperature. In this work, VACNT arrays were grown on chemically synthesized Fe_3O_4 NPs of diameter 6 nm by chemical vapor deposition. Coating the NPs with a thin layer of Al_2O_3 prior to CNT growth preserves the monodisperse sizes, resulting in uniform, thick and dense VACNT arrays. Comparison with uncoated NPs shows that the Al_2O_3 coating effectively prevents the catalyst NPs from sintering and coalescing, resulting in improved control over VACNT growth.

KEYWORDS: carbon nanotubes, nanoparticles, iron oxide, chemical vapor deposition, atomic layer deposition

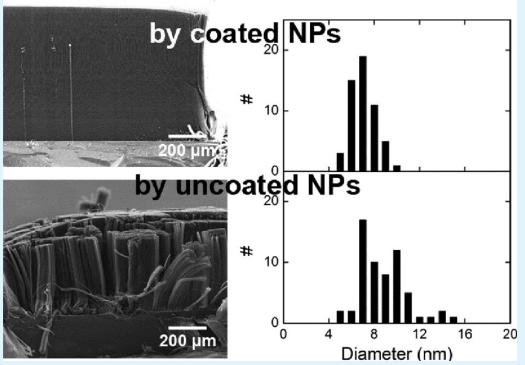

1. INTRODUCTION

The unique structural, mechanical, electrical, and thermal properties of carbon nanotubes (CNTs) have made them appealing for a wide range of scientific exploration and applications. Vertically aligned carbon nanotube (VACNT) arrays are ordered structures of CNTs where the nanotubes are oriented parallel to each other and perpendicular to a substrate. VACNT arrays containing a high density of long aligned CNTs have been used as building blocks of high-specific-strength fibers,[1] composites,[2] energy-absorbing foams,[3,4] and biomimetic scaffolds.[5] VACNTs are usually grown on substrate-supported metal nanoparticles (NPs) by chemical vapor deposition (CVD), which is a widely used chemical process to produce high-purity solid materials or thin film-coated surfaces.[6] A typical CVD process for CNT growth involves flowing a carbon gas precursor that decomposes on the catalyst particles and then nucleate and grow CNTs. Various types of catalytic NPs have been reported for growing VACNT arrays using CVD. Recently ligand-stabilized NPs, such as Fe, Ni, Co, have attracted extensive research interest.[7] In addition to their novel magnetic properties,[8−10] these NPs have been successfully used as catalysts for CNT growth[11,12] and carbon nanofiber growth.[13]

Achieving sustained and uniform growth of VACNT arrays is critical to realizing the potential of CNTs in advanced applications.[14] An important issue impeding such growth is the limited thermal stability of the NPs. At high growth temperatures (usually 700−800 °C), small catalyst NPs tend to agglomerate into larger particles through atomic interdiffusion, which is well-known as "Ostwald ripening". Previous studies showed that the resultant large catalyst particles created through Ostwald ripening tended to terminate VACNT growth[15] and catalyzed the growth of randomly oriented CNTs on the substrate.[16] Significant effort has been invested in resolving this issue by improving the thermal stability of catalyst NPs through several approaches, such as designing intermetallic alloys,[17] using prepatterned porous anodic alumina[18] or block copolymer micelles[19] as templates, and adding water vapor to the growth chamber.[20] However, an efficient and direct solution to the catalyst agglomeration is needed. Atomic layer deposition (ALD) is a method to deposit conformal thin films with atomic thickness control through self-limiting surface reactions.[21] As distinct from other CVD techniques, in ALD the source vapors are introduced onto the substrate alternately, separated by inert gas purging or evacuation periods, and react with the surface one at a time in a sequential manner.[22] ALD of metal oxide thin films has been reported as a method for stabilizing catalyst NPs at high temperatures,[23] and for performing heat treatment of FePt NPs, whereas preventing their agglomeration and coalescence.[24,25]

In this work, we report the stabilization of monodisperse Fe_3O_4 NPs with Al_2O_3 by ALD, which resulted in the synthesis of long VACNT arrays with a high degree of uniformity. Our results revealed significant effects of the Al_2O_3 coating on the size distribution, activity and lifetime of the Fe_3O_4 NPs. The ultrathin Al_2O_3 layer encapsulating the NPs prohibited their agglomeration at high temperatures, resulting in long, uniform, and dense VACNT arrays. Under the same conditions, the bare NPs fused into large particles and formed large areas of particle clusters, which catalyzed the growth of short, nonuniform and low-density CNT arrays.

Received: August 12, 2011
Accepted: October 10, 2011
Published: October 10, 2011

dx.doi.org/10.1021/am201082m | *ACS Appl. Mater. Interfaces* 2011, 3, 4180–4184

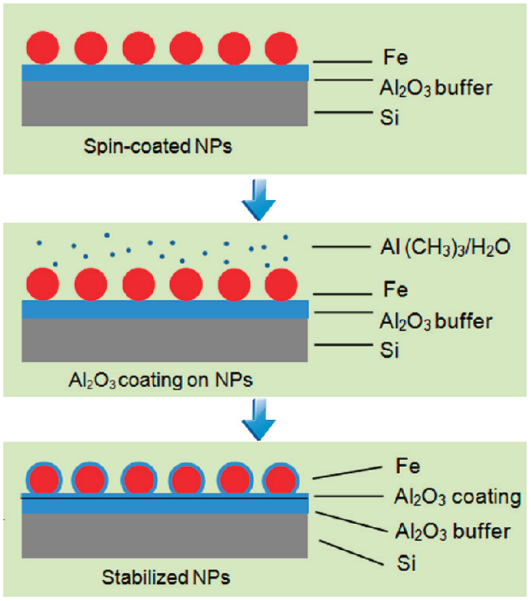

Figure 1. Schematic representation of Al_2O_3 ALD coating on monodispersed NPs.

2. EXPERIMENTAL SECTION

Iron Oxide Nanoparticle Synthesis and Characterization. Fe_3O_4 NPs with an average diameter of 6 nm were synthesized using a method reported by Woo et al.[26] Four hundred microliters (3.04 mmol) of $Fe(CO)_5$ (99.5%, Alfa Aesar) was rapidly injected into a solution containing 0.96 mL (3.04 mmol) of oleic acid (99%, Alfa Aesar) and 20 mL of octyl ether (TCI America) in a 100 mL three-necked, round-bottomed flask at 100 °C under nitrogen flow. The solution was then slowly heated and refluxed for 2 h at ~300 °C. Upon cooling, ethanol was added (1 mL per mL of NP growth solution), and the NPs were isolated by centrifugation. The NPs were resuspended in hexanes (~1 wt %) and were then spincast on ALD Al_2O_3 buffer layer (~10 nm)/Si substrate with an approximate monolayer coverage.[27] Transmission electron microscopy (TEM) images of the NPs dropcast onto a Cu TEM grid with the amorphous carbon and Formvar supports were acquired using a JEOL 2000FX TEM operated at 200 kV. The NP sizes were measured using the ImageJ software. For each NP sample, the diameter and standard deviation were determined by averaging measurements of 100 NPs.

Al_2O_3 Coating and VACNT Array Growth. ALD was carried out following the procedure described by Gong, et al.[28] Ten cycles of trimethylaluminum (TMA)/H_2O deposited a 1 nm Al_2O_3 layer onto the NP-coated substrate. CNTs were grown from the Al_2O_3 coated Fe_3O_4/Al_2O_3/Si substrates using CVD. Fe_3O_4 NPs with and without Al_2O_3 coating were placed at equivalent positions in the same CVD furnace during the same run. After loading the catalysts, the growth tube was evacuated to 25 Torr and refilled with a mixture of flowing H_2 (10 standard cubic centimeters per min, sccm) and Ar (65 sccm). The furnace was heated to 750 °C in approximately 10 min. The carbon precursor, ethylene (C_2H_4), was introduced into the growth tube at a flow rate of 15 sccm once the furnace reached 750 °C, which marked the beginning of the growth time. A series of identical catalyst samples were used to grow VACNT arrays with growth times of 5, 10, 20, 30, and 40 min. The array height was measured using a calibrated scale bar in an optical microscope (30 ×).

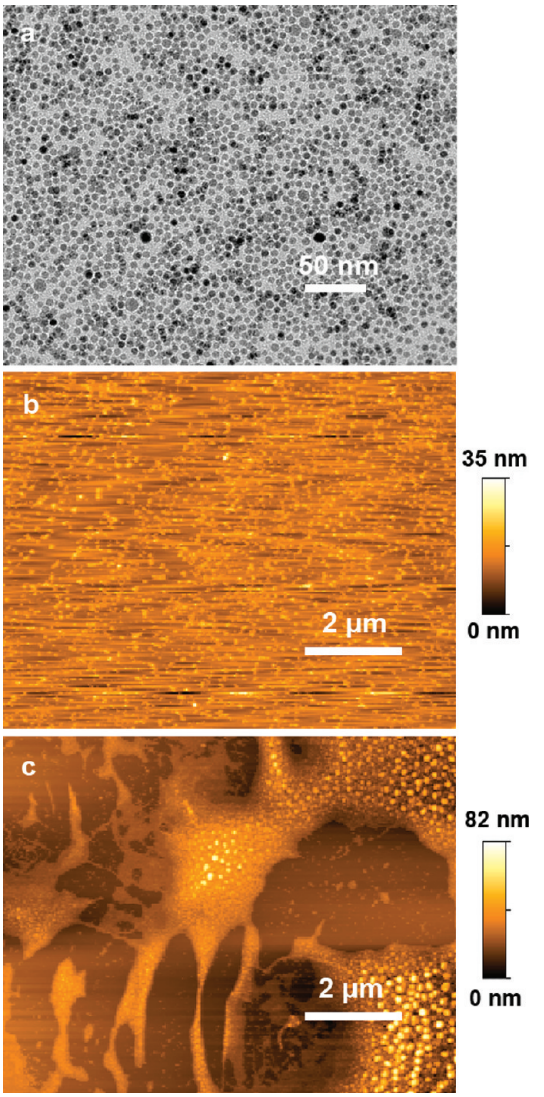

Figure 2. (a) TEM image of the as-synthesized Fe_3O_4 NPs; AFM images of (b) Fe_3O_4 NPs with Al_2O_3 ALD coating and (c) bare NPs, after annealing for 10 min under a H_2/Ar atmosphere from room temperature to 750 °C.

The morphology of the CNT arrays was investigated using a field emission scanning electron microscope (FE-SEM) (JEOL 6400) operated at 5 kV, and the quality of the VACNT arrays was examined by a Renishaw Raman spectrometer using a 514 nm laser. The CNT diameter was measured using a JEOL 2010F TEM operated at 200 kV. To characterize the pregrowth process, samples of Fe_3O_4 NPs with and without the Al_2O_3 coating were exposed to the CNT growth environment in the absence of C_2H_4. The samples were cooled to room temperature immediately after reaching 750 °C. The annealed samples were then imaged by atomic force microscopy (AFM, Veeco Caliber) using silicon nanoprobe cantilevers as scanning probes. The noncontact scanning mode was used to collect images at a voltage set point of 2.8 V and a scan rate of 0.5−1 Hz.

3. RESULTS AND DISCUSSION

The process for stabilizing NPs by coating with Al_2O_3 through ALD is depicted in Figure 1. During spincasting, the ligands keep the NPs well separated and prevent agglomeration of the NP

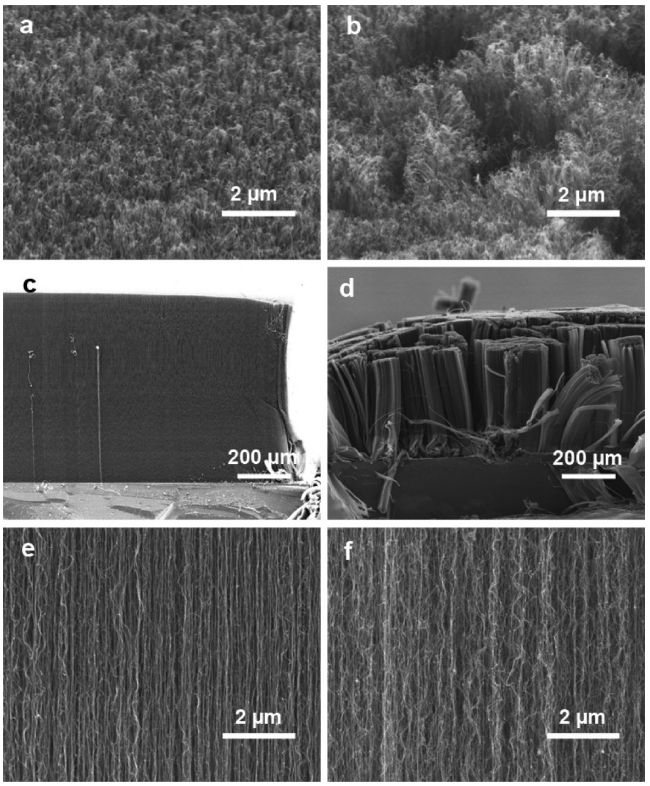

Figure 3. SEM images of top views of VACNT arrays grown from the (a) Al_2O_3-coated NPs and (b) bare NPs with 40 min growth, and side views of the CNT arrays grown from the (c) Al_2O_3-coated NPs and (d) bare NPs with 40 min growth. Further magnified SEM images of cross-sections of the CNT arrays grown from (e) Al_2O_3-coated NPs and from (f) bare NPs.

cores, which have average diameters of 6 nm, as shown in Figure 2a. After ligand removal from the catalyst NPs by ultraviolet light and ozone (UVO) for 5 min, ALD of an amorphous, 1 nm thick layer of Al_2O_3 provided a significant barrier to mobility of the underlying NPs. Conformal Al_2O_3 coatings produced by ALD have been found to fully encapsulate NPs.[29,30] In addition, ALD films are usually deposited uniformly on substrates that have the same chemical composition.[31] The oleic acid coating on the NPs results in gaps between NP cores of ~2−3 nm. After removing the ligands, we anticipate that the Al_2O_3 is deposited, on top of the NPs, on the buffer layer supporting the NPs, and within the gaps between NPs.

Pregrowth experiments performed in the absence of the carbon precursor allowed for characterization of the ripening phenomena. Typical AFM images in Figure 2 reveal striking differences in the wetting behavior of the two types of Fe_3O_4 catalysts. As shown in Figure 2b, the coated sample exhibited monodisperse NPs with a narrow size distribution. In comparison, Figure 2c showed that the bare NPs coarsened into larger NPs that formed agglomerates, between which few discrete NPs were present. These observations are supported by the variation in the surface roughness, which was approximately 12 nm for the coated NPs and approximately 35 nm for the bare NPs after pregrowth treatment. The Al_2O_3 coating appears to impede wetting of the Fe_3O_4 NPs on the substrate surface at high temperatures. VACNTs reported in this work grow through root-type growth. While the Al_2O_3 layer immobilizes the catalyst

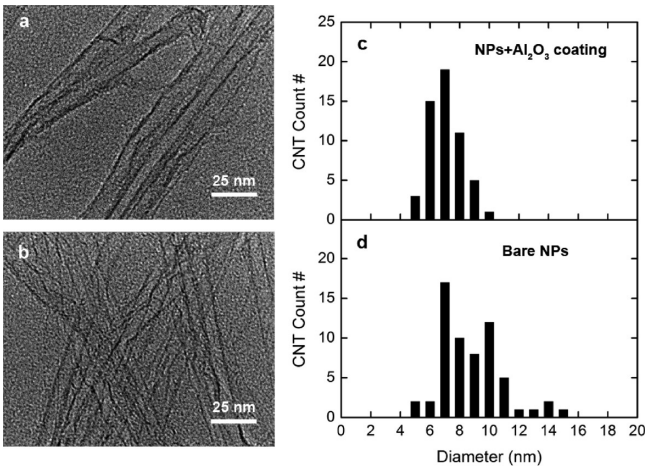

Figure 4. TEM images of CNTs grown from the (a) Al_2O_3-coated NPs and (b) bare NPs. Corresponding histograms of the CNT diameters, measured from TEM images acquired for at least 30 nanotubes in each sample, are plotted in (c) and (d), respectively.

NPs, it does not quench their catalytic activity toward CNT growth. It is plausible that gaps in the shell large enough to support CNT growth may exist, or melting of the encapsulated NPs might allow a gap to open if parts of the Al_2O_3 float at the interface. Moreover, at temperatures of ~700−800 °C, the amorphous Al_2O_3 is expected to crystallize into γ-Al_2O_3,[24,32] giving rise to morphological changes.[24] Through one of these mechanisms, the ultrathin coating on the NPs might migrate into the thicker buffer layer during the heating, leaving the catalyst surface uncovered for CNT growth. In contrast, the mobility of uncoated NPs significantly increased, resulting in severe particle agglomeration.

The ripening behavior and the catalyst morphology after pregrowth closely correlate with the VACNT array morphology (Figure 3). Top views of the arrays grown from the Al_2O_3-coated NPs (Figure 3a) revealed a more regular array surface than for the arrays grown using bare NPs (Figure 3b). Side views of the VACNT arrays also show distinctly different morphologies: uniform, thick and dense arrays (Figure 3c) were produced by the coated NPs; while short, disordered and sparse arrays (Figure 3d) resulted from the bare NPs. Further magnification of the SEM images showed that the CNTs grown from the coated NPs were straight and highly densely packed (Figure 3e), while the CNTs grown using bare NPs were irregularly coiled, forming a loose structure (Figure 3f).

Al_2O_3-coated catalyst NPs gave rise to uniformly distributed CNTs in the array. Measurements from TEM images (Figure 4a,b) revealed that the CNTs obtained from the coated NPs had diameters of 7 ± 1 nm, while the CNTs grown from the bare NPs had diameters of 9 ± 2 nm. The CNTs grown from the coated NPs have a narrower diameter dispersion (Figure 4c) than those synthesized from the bare NPs (Figure 4d). Measurement of the catalyst morphology prior to growth and the resulting CNT arrays suggest that the CNT growth conforms to a well-known mechanism: the NPs catalytically decompose C_2H_4 into atomic carbon, which dissolves in the NPs and is precipitated out as CNTs with diameters close to size of the monodisperse catalyst NPs.[33] In comparison, unencapsulated NPs resulted in a broad NP size distribution through agglomeration and coalescence. Only those NPs with suitably small sizes

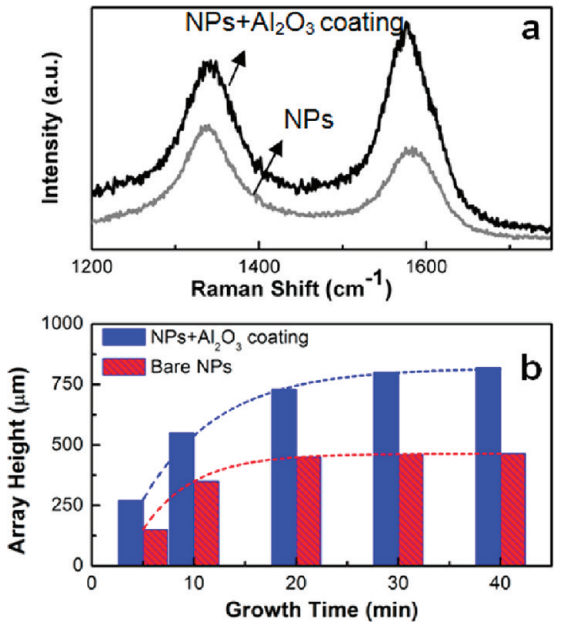

Figure 5. (a) Comparison of Raman spectra of VACNT arrays produced by Al_2O_3-coated NPs and bare NPs. (b) Plots of maximum height (histogram) of CNT arrays grown by Al_2O_3-coated NPs and bare NPs, as a function of time. The dotted line indicates excellent curve fitting of the experimental data to Iijima's growth equation.[34]

catalyzed CNT growth, and the larger NPs were too large to catalyze nanotube growth, resulting in gaps between aligned CNT bundles.

The Raman spectra in Figure 5a suggest that the Al_2O_3-coated NPs produced CNTs with greater crystallinity, fewer defects and less amorphous carbon. The CNT quality can be characterized by the intensity ratio (I_G/I_D) of the G-band peak (1585 cm^{-1}) to the D-band peak (1350 cm^{-1}). The G-band peak arises from crystalline carbon bonds, and the D-band peak corresponds to amorphous carbon. Figure 5a shows that CNTs synthesized from the coated NPs have a larger I_G/I_D ratio than for CNTs grown from the bare NPs.

As shown in Figure 5b, the catalytic activity and lifetime of the NPs strongly depend on whether the Al_2O_3 coating is present. The growth rate of the VACNT array represents the catalytic activity, and the time at which VACNT growth ceases is the lifetime. A comparison of the VACNT array height vs time plots showed that the coated NPs produced approximately 820 μm arrays in 40 min at a fast initial growth rate of 55 μm/min, whereas the bare NPs produced 450 μm arrays in 20 min at a slower initial growth rate of 32 μm/min. Longer growth times yielded a final height of 830 μm for coated NPs and 470 μm for the uncoated NPs. In summary, the catalytic activity and lifetime of the bare NPs were about 60% of the values obtained from the coated NPs. The time-dependent progression of the growth (assessed by fitting the height vs time curves) is in good agreement with Iijima's growth models.[34]

Our simple, template-free approach imparts thermal stability and thus produces uniformly distributed, long VACNT arrays. Compared with previously reported long VACNTs[35] grown by Al_2O_3/Fe catalyst, which was prepared by an ion-beam assisted deposition technique, the VACNTs were successfully grown by chemically synthesized NPs in this study. The chemical synthetic approach allows fast preparation of small and monodisperse catalyst NPs and in future work complex patterns of VACNTs might be enabled by patterning of these catalyst NPs.[13] In addition, the chemical approach of synthesizing NPs is more conducive to large-scale and low cost production. ALD-based stabilization of catalytic NPs is also promising for VACNT synthesis on large substrates. Such VACNT arrays have a wide range of applications. For example, the ultrahigh surface area coupled with good electrical conductivity (118 S/cm for a shear-pressed array[2]) may enable their use as components in solar cells[36] or supercapacitors.[37] The high strength and lightweight also may make them ideal reinforcement for polymeric composites.[2]

4. CONCLUSION

Sub-millimeter-long VACNT arrays were successfully grown from chemically synthesized catalyst NPs. Here, we have demonstrated a simple and effective method to significantly enhance the thermal stability of monodispersed NPs, maintaining their monodisperse sizes at high temperatures. An ultrathin Al_2O_3 ALD coating deposited directly onto the NPs serves as an encapsulating layer to prevent the NPs from agglomeration, which results in highly uniform VACNT arrays, where the CNT diameter corresponds to the catalyst NP size. The improved uniformity and quality of the CNT arrays due to the Al_2O_3 ALD coating will improve their performance in applications that require high surface area and porosity, lightweight, or high strength and electrical conductivity.

AUTHOR INFORMATION

Corresponding Author

*Tel: 919-513-0559. E-mail: ytzhu@ncsu.edu.

ACKNOWLEDGMENT

This work was sponsored by a NC Space Grant and the National Science Foundation (CBET-0967559). We thank Weizong Xu and Yong-jae Choi for their help with the microscopy measurements. We also thank Prof. Jon-Paul Maria for helpful discussions.

REFERENCES

(1) Zhang, X. F.; Li, Q.; Holesinger, T. G.; Arendt, P. N.; Huang, J. Y.; Kirven, P. D.; Clapp, T. G.; DePaula, R. F.; Liao, X. Z.; Zhao, Y. H.; Zheng, L. X.; Peterson, D. E.; Zhu, Y. T. *Adv. Mater.* **2007**, *19*, 4198–4201.

(2) Bradford, P. D.; Wang, X.; Zhao, H.; Maria, J.; Jia, Q.; Zhu, Y. T. *Compos. Sci. Technol.* **2010**, *70*, 1980.

(3) Cao, A. Y.; Dickrell, P. L.; Sawyer, W. G.; Ghasemi-Nejhad, M. N.; Ajayan, P. M. *Science* **2005**, *310*, 1307–1310.

(4) Bradford, P. D.; Wang, X.; Zhao, H.; Zhu, Y. T. *Carbon* **2011**, *49*, 2834–2841.

(5) Correa-Duarte, M. A.; Wagner, N.; Rojas-Chapana, J.; Morsczeck, C.; Thie, M.; Giersig, M. *Nano Lett.* **2004**, *4*, 2233–2236.

(6) Park, J. H.; Sudarshan, T. S. *Chemical Vapor Deposition*; Surface Engineering Series; ASM International: Materials Park, OH, 2001; Vol. 2.

(7) Park, J.; Joo, J.; Kwon, S. G.; Jang, Y.; Hyeon, T. *Angew. Chem., Int. Ed.* **2007**, *46*, 4630–4660.

(8) Leslie-Pelecky, D. L.; Rieke, R. D. *Chem. Mater.* **1996**, *8*, 1770–1783.

(9) Majetich, S. A.; Sachan, M. *J. Phys. D: Appl. Phys.* **2006**, *39*, R407.

(10) Bedanta, S.; Kleemann, W. *J. Phys. D: Appl. Phys.* **2009**, *42*, 013001.

(11) Choi, G.; Cho, Y.; Son, K.; Kim, D. *Microelectron. Eng.* **2003**, *66*, 77–82.
(12) Paillet, M.; Jourdain, V.; Poncharal, P.; Sauvajol, J. L.; Zahab, A.; Meyer, J. C.; Roth, S.; Cordente, N.; Amiens, C.; Chaudret, B. *J. Phys. Chem. B* **2004**, *108*, 17112–17118.
(13) Sarac, M. F.; Wilson, R. M.; Johnston-Peck, A. C.; Wang, J.; Pearce, R.; Klein, K. L.; Melechko, A. V.; Tracy, J. B. *ACS Appl. Mater. Interfaces* **2011**, *4*, 936–940.
(14) Hinds, B. J.; Chopra, N.; Rantell, T.; Andrews, R.; Gavalas, V.; Bachas, L. G. *Science* **2004**, *303*, 62–65.
(15) Amama, P. B.; Pint, C. L.; Kim, S. M.; McJilton, L.; Eyink, K. G.; Stach, E. A.; Hauge, R. H.; Maruyama, B. *ACS Nano* **2010**, *4*, 895–904.
(16) Homma, Y.; Yamashita, T.; Finnie, P.; Tomita, M.; Ogino, T. *Jpn. J. Appl. Phys.* **2002**, *41*, 89–91.
(17) Zhao, H.; Bradford, P. D.; Wang, X.; Liu, W.; Luo, T. J. M.; Jia, Q.; Zhu, Y.; Yuan, F. G. *Mater. Lett.* **2010**, *64*, 1947–1950.
(18) Bae, E. J.; Choi, W. B.; Jeong, K. S.; Chu, J. U.; Park, G. S.; Song, S.; Yoo, I. K. *Adv. Mater.* **2002**, *14*, 277.
(19) Bennett, R. D.; Xiong, G. Y.; Ren, Z. F.; Cohen, R. E. *Chem. Mater.* **2004**, *16*, 5589–5595.
(20) Amama, P. B.; Pint, C. L.; McJilton, L.; Kim, S. M.; Stach, E. A.; Murray, P. T.; Hauge, R. H.; Maruyama, B. *Nano Lett.* **2008**, *9*, 44–49.
(21) Klaus, J. W.; Sneh, O.; George, S. M. *Science* **1997**, *278*, 1934.
(22) Ritala, M.; Leskela, M. In *Handbook of Thin Film Materials*; Academic Press: New York, 2001; Vol. 1, p 103.
(23) Whitney, A. V.; Elam, J. W.; Stair, P. C.; Van Duyne, R. P. *J. Phys. Chem. C* **2007**, *111*, 16827–16832.
(24) Johnston-Peck, A. C.; Giovanna, S.; Wang, J.; Parsons, G. N.; Tracy, J. B. *Nanoscale* **2011**, *3*, 4142−4149.
(25) Kong, J. Z.; Gong, Y. P.; Li, X. F.; Li, A. D.; Zhang, J. L.; Yan, Q. Y. *J. Mater. Chem.* **2011**, *21*, 5046–5050.
(26) Woo, K.; Hong, J.; Choi, S.; Lee, H. W.; Ahn, J. P.; Kim, C. S.; Lee, S. W. *Chem. Mater.* **2004**, *16*, 2814–2818.
(27) Johnston-Peck, A. C.; Wang, J.; Tracy, J. B. *Langmuir* **2011**, *8*, 5040–5046.
(28) Gong, B.; Peng, Q.; Parsons, G. N. *J. Phys. Chem. B* **2011**, *19*, 5930–5938.
(29) Ferguson, J. D.; Weimer, A. W.; George, S. M. *Thin Solid Films* **2000**, *371*, 95–104.
(30) Scott, I. D.; Jung, Y. S.; Cavanagh, A. S.; Yan, Y.; Dillon, A. C.; George, S. M.; Lee, S. *Nano Lett.* **2011**, *11*, 414–418.
(31) Puurunen, R. L.; Vandervorst, W.; Besling, W. F. A.; Richard, O.; Bender, H.; Conard, T.; Zhao, C.; Delabie, A.; Caymax, M.; De Gendt, S. *J. Appl. Phys.* **2004**, *96*, 4878.
(32) Cao, S.; Pedraza, A. J.; Lowndes, D. H.; Allard, L. F. *Appl. Phys. Lett.* **1994**, *65*, 2940–2942.
(33) Cheung, C. L.; Kurtz, A.; Park, H.; Lieber, C. M. *J. Phys. Chem. B* **2002**, *106*, 2429–2433.
(34) Futaba, D. N.; Hata, K.; Yamada, T.; Mizuno, K.; Yumura, M.; Iijima, S. *Phys. Rev. Lett.* **2005**, *95*, 056104.
(35) Li, Q. W.; Zhang, X. F.; DePaula, R. F.; Zheng, L. X.; Zhao, Y. H.; Stan, L.; Holesinger, T. G.; Arendt, P. N.; Peterson, D. E.; Zhu, Y. T. *Adv. Mater.* **2006**, *18*, 3160–3163.
(36) Kongkanand, A.; Domínguez, R. M.; Kamat, P. V. *Nano Lett.* **2007**, *7*, 676–680.
(37) Zhang, H.; Cao, G.; Wang, Z.; Yang, Y.; Shi, Z.; Gu, Z. *Nano Lett.* **2008**, *8*, 2664–2668.